

Characterization of the Chloranilate($\bullet 3^-$) π Radical as a Strong Spin-Coupling Bridging Ligand

Kil Sik Min,[†] Arnold L. Rheingold,[‡] Antonio DiPasquale,[‡] and Joel S. Miller^{*†}

Department of Chemistry, University of Utah, 315 South 1400 East, Room 2124, Salt Lake City, Utah 84112-0850, and Department of Chemistry, University of California, San Diego, La Jolla, California 92093-0358

Received June 14, 2006

Dinuclear [(TPA)Co^{II}(CA²⁻)Co^{II}(TPA)](BF₄)₂·2MeOH (**1**) [TPA = tris(2-pyridylmethyl)amine] and [(TPA)Co^{II}(CA^{•3-})Co^{II}(TPA)](BF₄)₂·2Et₂O (**2**) with a bridging chloranilate radical ligand formed by reduction of **1** are crystallographically and magnetically characterized. **1** has shown a weak antiferromagnetic coupling within the Co^{II} dimer [$J/k_B = -0.65$ K (-0.45 cm⁻¹)], while **2** has a 2 orders of magnitude stronger antiferromagnetic interaction between the Co^{II} ion and a radical [$J/k_B = -75$ K (52 cm⁻¹)].

Molecule-based materials containing organic radicals have attracted considerable interest for the development of organic-based magnets¹ as well as valence tautomerism² and mixed-valence materials.³ Metal complexes with 1,4-dihydroxybenzoquinonediide, chloranilate (CA²⁻), ligands have been widely studied because they are good building blocks to make extended network structures because they can coordinate in a bis-bidentate manner.⁴ However, metal compounds with the CA ligand as a radical, and consequently their spin-coupling ability, have yet to be described, although two dinuclear Co^{III} complexes with the DHBQ^{•3-} (DHBQ = deprotonated 2,5-dihydroxy-1,4-benzoquinone) radical have recently been reported.⁵ Herein, we report the formation of [(TPA)Co^{II}(CA²⁻)Co^{II}(TPA)](BF₄)₂·2MeOH (**1**) [TPA = tris(2-pyridylmethyl)amine] and its monoreduced species

[(TPA)Co^{II}(CA^{•3-})Co^{II}(TPA)](BF₄)₂·2Et₂O (**2**), revealing that the CA^{•3-} trianion radical strongly spin couples with two high-spin $S = 3/2$ Co^{II} ions.

1 was prepared from the reaction of Co(BF₄)₂, TPA, and CA in an inert-atmosphere glovebox.⁶ Dark-red **2** was prepared by the one-electron reduction of **1** with CoCp₂.⁷ Compound **2** can be formulated as either mixed-valent [(TPA)Co^I(CA²⁻)Co^{II}(TPA)]⁺ or [(TPA)Co^{II}(CA^{•3-})Co^{II}(TPA)]⁺ containing CA^{•3-}. In the cyclic voltammogram, the reduction potential ($E_{1/2}$) from **1** to **2** was at -1.04 V vs Fc/Fc⁺ couple; thus, **1** can be reduced to **2** easily by CoCp₂ (CoCp₂/CoCp₂⁺, $E_{1/2} = -1.33$ V).

Red-brown block-shaped crystals of **1** and **2** suitable for X-ray crystal analysis were obtained by allowing the reaction mixture to stand for several days without agitation or via diffusion with diethyl ether. The structures of the cations of **1** and **2** (Figure 1)⁸ display a distorted octahedral geometry by coordinating with the four N atoms of TPA and the two O atoms of CA in the cis positions. Both **1** and **2** possess

(6) To a MeOH solution (10 mL) of Co(BF₄)₂·6H₂O (234 mg, 0.688 mmol) was added a MeOH solution (10 mL) of TPA (200 mg, 0.688 mmol) and a MeOH solution of chloranilic acid (H₂CA; 72 mg, 0.344 mmol) in a wet box (<1 ppm O₂). The color of the mixture resulted in a dark-red and then a dark-red-brown solution. Triethylamine (0.1 mL, 0.688 mmol) was added to the mixture for neutralization, which gives rise to a red-brown solution. Then the solution was heated to reflux for 30 min. The solution was allowed to stand at room temperature overnight, whereupon dark-red-brown crystals formed, which were collected by filtration, washed with MeOH, and dried in vacuo to afford 257 mg (65%) of **1**. Anal. Calcd for C₄₄H₄₄B₂Cl₂·C₂F₈N₈O₆: C, 46.22; H, 3.88; N, 9.80. Found: C, 46.25; H, 3.85; N, 9.96. FT-IR (KBr): ν_{CH} 3082 (w), 2919 (w), 1609 (s), ν_{CO} 1526 (vs), 1484 (s), 1438 (s), 1379 (s), 1291 (m), 1060 (m, br), 851 (s), 771 (s) cm⁻¹. Absorption spectrum (CH₂Cl₂): λ_{max} , nm (ϵ_M , L mol⁻¹ cm⁻¹): 390 (5.5×10^3), 537 (8.3×10^2).

(7) To an MeCN solution (5 mL) of **1** (50 mg, 0.044 mmol) was added an MeCN solution (5 mL) of CoCp₂ (8.3 mg, 0.044 mmol) in a drybox (<1 ppm O₂). The color turned dark red. The solution was stirred for 1 h at room temperature. Red-brown block-shaped crystals of **2** were obtained by solvent diffusion of diethyl ether into the reaction mixture of acetonitrile for 2 or 3 days and then were collected by filtration, washed with MeCN, and dried in vacuo (yield: 40 mg, 80%). FT-IR (KBr): ν_{CH} 3065 (w), 2926 (w), 1604 (s), 1534 (w), 1481 (s), ν_{CO} 1442 (vs), 1264 (m), 1055 (m, br), 832 (s), 773 (s) cm⁻¹. Absorption spectrum (MeCN): λ_{max} , nm (ϵ_M , L mol⁻¹ cm⁻¹): 247 (1.8×10^4), 330 (1.2×10^4), 484 (6.8×10^3), 562 (sh, 3.3×10^3), 738 (2.5×10^3). This compound is very sensitive to air.

* To whom correspondence should be addressed. E-mail: jsmiller@chem.utah.edu. Tel: 1 801 5855455. Fax: 1 801 5818433.

[†] University of Utah.

[‡] University of California, San Diego.

- (1) (a) Manriquez, J. M.; Yee, G. T.; McLean, R. S.; Epstein, A. J.; Miller, J. S. *Science* **1991**, *252*, 1415. (b) Kahn, O. *Adv. Inorg. Chem.* **1995**, *43*, 179. (c) Ohtsu, H.; Tanaka, K. *Angew. Chem., Int. Ed.* **2004**, *43*, 6301. (d) Siri, O.; Taquet, J.-P.; Collin, J.-P.; Rohmer, M.-M.; Bénard, M.; Braunstein, P. *Chem.—Eur. J.* **2005**, *11*, 7247.
- (2) (a) Shultz, D. A. In *Magnetism—Molecules to Materials*; Miller, J. S., Drillon, M., Eds.; Wiley-VCH: Weinheim, Germany, 2001; Vol. 2, p 281. (b) Dei, A.; Gatteschi, D.; Sangregorio, C.; Sorace, L. *Acc. Chem. Res.* **2004**, *37*, 827.
- (3) Demadis, K. D.; Hartshorn, C. M.; Meyer, T. J. *Chem. Rev.* **2001**, *101*, 2655.
- (4) Kitagawa, S.; Kawata, S. *Coord. Chem. Rev.* **2002**, *224*, 11.
- (5) (a) Carbonera, C.; Dei, A.; Létard, J.-F.; Sangregorio, C.; Sorace, L. *Angew. Chem., Int. Ed.* **2004**, *43*, 3136. (b) Tao, J.; Maruyama, H.; Sato, O. *J. Am. Chem. Soc.* **2006**, *128*, 1790.

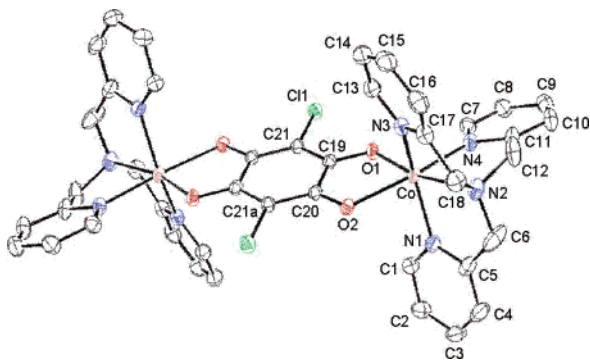


Figure 1. Structure of the monocation $[(\text{TPA})\text{Co}^{\text{II}}(\text{CA}^{*3-})\text{Co}^{\text{II}}(\text{TPA})]^+$ in crystals of **2**. The atoms are represented by 30% probable thermal ellipsoids. That of the dication in crystals of **1** is similar and not shown. H atoms, solvent, and $[\text{BF}_4]^-$ are omitted for clarity. Relevant distances (Å) and angles (deg): for **1**, Co–O1 2.030(2), Co–O2 2.277(3), Co–N1 2.110(3), Co–N2 2.239(3), Co–N3 2.080(3), Co–N4 2.108(3), C19–O1 1.266(4), C20–O2 1.246(4), C19–C20 1.527(5), C19–C21 1.372(5), C20–C21a 1.409(5), C21–C11 1.729(4), O1–Co–O2 74.29(9), N1–Co–N2 76.09(11), N2–Co–N3 77.61(11), N2–Co–N4 75.81(12); for **2**, Co–O1 1.978(2), Co–O2 2.166(2), Co–N1 2.085(2), Co–N2 2.262(2), Co–N3 2.090(2), Co–N4 2.109(2), C19–O1 1.304(3), C20–O2 1.282(2), C19–C20 1.473(3), C19–C21 1.386(3), C20–C21a 1.400(3), C21–C11 1.743(2), O1–Co–O2 79.62(7), N1–Co–N2 77.43(9), N2–Co–N3 76.06(8), N2–Co–N4 77.20(9).

crystallographic centers of symmetry, and average Co–O and Co–N bond distances are 2.106(2) and 2.134(2) Å and 2.072(1) and 2.137(1) Å for **1** and **2**, respectively. Interestingly, the average Co–L bond lengths are very similar to each other [Co–L_{av} = 2.122(1) Å for **1** and 2.115(1) Å for **2**] and indicate that the oxidation state of the Co ion in **2** is 2+, as is the Co ion in **1**. Thus, the $[(\text{TPA})\text{Co}^{\text{I}}(\text{CA}^{2-})\text{Co}^{\text{II}}(\text{TPA})]^+$ formulation for **2** can be excluded. Furthermore, the average C–O bond distance [1.256(3) Å] of **1** is shorter than that of **2** [1.293(1) Å], while the C19–C20 bonds of **1** are longer than those of **2** by 0.054 Å. The significant difference is attributed to the reduction of CA^{2-} to CA^{*3-} by CoCp_2 . Additionally, the very strong peak at 1526 cm^{-1} for **1** shifts to 1442 cm^{-1} upon reduction, indicating that CA^{2-} in **1** is reduced to CA^{*3-} in **2**, and a metal-centered reduction does not occur.

The pyridyl groups of TPA ligands in **1** and **2** are involved in offset π – π -stacking interactions⁹ between the Co^{II} dimers, in which both complexes give rise to 1-D supramolecular network structures.

While several metal(II/III) dimers with bridged CA^{2-} have been reported,^{4,10} however, this is the first example with the radical bridging the two spin-bearing metal sites. Thus, the

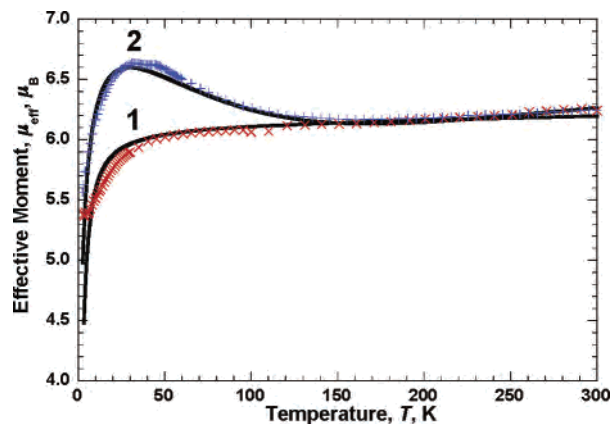


Figure 2. $\mu_{\text{eff}}(T)$ for **1** (×) and **2** (+). The solid lines are the best-fit curves to eqs 1 and 2, respectively.

magnetic properties of the $[(\text{TPA})\text{Co}^{\text{II}}(\text{CA}^{*3-})\text{Co}^{\text{II}}(\text{TPA})]^+$ cation were characterized to ascertain the spin coupling (J) between Co^{II} and CA^{*3-} as well as for the presence of valence tautomerism and/or spin-crossover behavior(s).

Variable-temperature 2–300 K magnetic susceptibility, χ , measurements on solid samples of **1** and **2** have been performed on a SQUID magnetometer (external field 1000 Oe). For complex **1**, at room temperature, the effective moment, $\mu_{\text{eff}} [= (8\chi T)^{1/2}]$, is 6.26 $\mu_{\text{B}}/\text{Co}_2$, and $\mu_{\text{eff}}(T)$ decreases monotonically with decreasing temperature to 5.38 μ_{B} at 3 K (Figure 2), indicating a very weak antiferromagnetic interaction within the $\text{Co}^{\text{II}}(\text{CA}^{2-})\text{Co}^{\text{II}}$ unit. $\chi(T)$ for **1** was fit to an analytical expression, eq 1 ($H = -2JS_1 \cdot S_2$), for a coupled $S = 3/2$ dimer.¹¹ The best fit had J/k_{B} of -0.65 K (-0.45 cm^{-1}), $g = 2.24$, $\theta = -0.1$ K, and the temperature-independent paramagnetism, TIP = 4×10^{-4} emu mol^{-1} .¹² The weak interaction can be attributed to a long distance between the Co^{II} ions (8.089 Å)

$$\chi = [Ng^2\mu_{\text{B}}^2/k_{\text{B}}(T - \theta)]F(T) + \text{TIP} \quad (1)$$

where

$$F(T) = [2 \exp(2J/k_{\text{B}}T) + 10 \exp(6J/k_{\text{B}}T) + 28 \exp(12J/k_{\text{B}}T)]/[1 + 3 \exp(2J/k_{\text{B}}T) + 5 \exp(6J/k_{\text{B}}T) + 7 \exp(12J/k_{\text{B}}T)]$$

Complex **2** has a room temperature μ_{eff} of 6.20 $\mu_{\text{B}}/\text{Co}_2$; $\mu_{\text{eff}}(T)$ decreases slightly with a decrease in the temperature to 6.17 μ_{B} at 160 K, then gradually increases to a maximum of 6.63 μ_{B} at 32 K, and again decreases to 5.56 μ_{B} at 2 K (Figure 2), indicating a strong antiferromagnetic interaction within the three-spin-site $\text{Co}^{\text{II}}(\text{CA}^{*3-})\text{Co}^{\text{II}}$ unit. $\chi(T)$ for **2** was fit to eq 2 [$H = -2J(S_1 \cdot S_2 + S_2 \cdot S_3)$] for a linear three-spin system with $S_1 = S_3 = 3/2$ and $S_2 = 1/2$.¹³ The best fit had J/k_{B} of -75 K (-52 cm^{-1}), $g = 2.36$, $\theta = -2.6$ K, and TIP

(8) Crystal and structural refinement parameters for **1** and **2**: for **1**, $\text{C}_{44}\text{H}_{44}\text{B}_2\text{Cl}_2\text{Co}_2\text{F}_8\text{N}_8\text{O}_6$, fw = 1143.25 g mol^{-1} , monoclinic, space group $C2/c$, $a = 26.785(3)$ Å, $b = 10.884(1)$ Å, $c = 16.707(2)$ Å, $\beta = 92.832(2)^\circ$, $V = 4864.6(9)$ Å³, $Z = 4$, $d_{\text{calcd}} = 1.561$ g cm^{-3} , $\mu(\text{Mo K}\alpha) = 0.879$ mm^{-1} , $R1 = 0.0545$, $wR2 = 0.1399$; for **2**, $\text{C}_{50}\text{H}_{56}\text{BCl}_2\text{Co}_2\text{F}_4\text{N}_8\text{O}_6$, fw = 1140.60 g mol^{-1} , monoclinic, space group $P2/n$, $a = 13.846(7)$ Å, $b = 11.493(6)$ Å, $c = 15.958(8)$ Å, $\beta = 90.687(9)^\circ$, $V = 2539(2)$ Å³, $Z = 2$, $d_{\text{calcd}} = 1.492$ g cm^{-3} , $\mu(\text{Mo K}\alpha) = 0.831$ mm^{-1} , $R1 = 0.0469$, $wR2 = 0.1300$. Data were collected on a Bruker SMART automatic diffractometer using graphite-monochromated Mo K α ($\lambda = 0.71073$ Å) radiation. Structures were solved by direct methods (SIR-2004) and refined by full-matrix least-squares refinement using the SHELXL97 program.

(9) (a) Desiraju, G. R. *Crystal Engineering: The Design of Organic Solids*; Elsevier: New York, 1989; Chapter 4. (b) Shetty, A. S.; Zhang, J.; Moore, J. S. *J. Am. Chem. Soc.* **1996**, *118*, 1019.

(10) (a) Heinze, K.; Huttner, G.; Zsolnai, L.; Jacobi, A.; Schöber, P. *Chem. – Eur. J.* **1997**, *3*, 732. (b) Heinze, K.; Huttner, G.; Walter, O. *Eur. J. Inorg. Chem.* **1999**, 593.

(11) Duggan, D. M.; Hendrickson, D. N. *Inorg. Chem.* **1975**, *14*, 1944.

(12) The data were corrected for diamagnetic contributions and included for temperature-independent paramagnetism.

(13) Zhong, A. J.; Matsumoto, N.; Okawa, H.; Kida, S. *Inorg. Chem.* **1991**, *30*, 436.

$= 4 \times 10^{-4} \text{ emu mol}^{-1}$.¹² The strong antiferromagnetic interaction is attributed to the overlap of the singly occupied molecular π^* orbital of CA^{3-} and the t_{2g} orbitals of the Co^{II} ion. This interaction is 2 orders of magnitude stronger than the weak antiferromagnetic interaction (-0.65 K) between the Co^{II} ions

$$\chi = \{Ng^2\mu_B^2/k_B(T - \theta)\}F(T) + \text{TIP} \quad (2)$$

where

$$F(T) = [84 + 35 \exp(-J/k_B T) + 10 \exp(-2J/k_B T) + \exp(-3J/k_B T) + \exp(-5J/k_B T) + 10 \exp(-6J/k_B T) + 35 \exp(-7J/k_B T)]/[16 + 12 \exp(-J/k_B T) + 8 \exp(-2J/k_B T) + 4 \exp(-3J/k_B T) + 4 \exp(-5J/k_B T) + 8 \exp(-6J/k_B T) + 12 \exp(-7J/k_B T)]$$

In conclusion, $[(\text{TPA})\text{Co}^{\text{II}}(\text{CA}^{3-})\text{Co}^{\text{II}}(\text{TPA})]^+$ possessing $S = 1/2$ CA^{3-} has been characterized, and the presence of CA^{3-} enhances the spin coupling between the $S = 3/2$ Co^{II} centers by 2 orders of magnitude. Further studies on the magnetism and fabrication of new molecule-based materials containing different oxidation states exhibiting valence tautomerism and spin crossover are ongoing.

Acknowledgment. We appreciate the continued partial support by the U.S. Department of Energy Division of Material Science (Grant DE-FG03-93ER45504) and the U.S. Air Force Office of Scientific Research (Grant F49620-03-1-0175).

Supporting Information Available: X-ray crystallographic files for **1** and **2** in CIF format. This material is available free of charge via the Internet at <http://pubs.acs.org>.

IC061076K